RSC Advances

PAPER

View Article Online
View Journal | View Issue

Cite this: *RSC Adv.*, 2022, **12**, 16329

Comparative study on the pyrolysis behavior and pyrolysate characteristics of Fushun oil shale during anhydrous pyrolysis and sub/supercritical water pyrolysis

Yang Lu,[ab] Zhijing Wang,[ab] Zhiqin Kang,*[ab] Wei Li,[d] Dong Yang[ab] and Yangsheng Zhao[abc]

Injected steam can be converted to the sub/supercritical state during the *in situ* exploitation of oil shale. Thus, the pyrolysis behavior and pyrolysate characteristic of Fushun oil shale during anhydrous pyrolysis and sub/supercritical water pyrolysis were fully compared. The results revealed that the discharged oil yields from sub/supercritical water pyrolysis were 5.44 and 14.33 times that from anhydrous pyrolysis at 360 °C and 450 °C, which was due to the extraction and driving effect of sub/supercritical water. Also, sub/supercritical water could facilitate the discharge and migration of shale oil from the pores and channels. The H_2 and CO_2 yields in sub/supercritical water pyrolysis were higher than that in anhydrous pyrolysis, resulting from the water–gas shift reaction. The component of shale oil was dominated by saturated hydrocarbons in anhydrous pyrolysis, which accounted for 50–65%. In contrast, a large amount of asphaltenes and resins was formed during pyrolysis in sub/supercritical water due to the solvent effect and weak thermal cracking. The shale oil from anhydrous pyrolysis was lighter than that from sub/supercritical water pyrolysis. Sub/supercritical water reduced the geochemical characteristic indices and lowered the hydrocarbon generation potential and maturity of solid residuals, which can be attributed to the fact that more organic matter was depolymerized and released. The pyrolysate characteristic of oil shale in sub/supercritical water pyrolysis was controlled by multiple mechanisms, including solvent and driving effect, chemical hydrogen-donation and acid–base catalysis.

Received 8th April 2022
Accepted 18th May 2022

DOI: 10.1039/d2ra02282f

rsc.li/rsc-advances

Introduction

Oil shale is rich in the complexes of organic kerogen, which can be thermally converted to shale oil and gas.[1–3] Because it is similar to natural petroleum, shale oil is considered a promising alternative energy and supplementary resource.[4,5] China has the second largest oil shale reserves in the world, which is approximately 47.6 billion tons (converted into shale oil).[6,7] Thus, realizing high-efficient exploitation of oil shale is conducive to meeting China's energy demand and alleviating its dependence on imports. The ways to obtain shale oil from oil shale include pyrolysis in a retorting furnace and *in situ* conversion.[8–10] The method of pyrolysis in a retorting furnace has high exploitation and equipment costs, low utilization efficiency and causes serious environmental pollution. Thus, based on these issues, Zhao's team from Taiyuan University of Technology proposed *in situ* steam injection technology for oil shale exploitation, achieving significant progress.[11–13] When superheated steam is injected over 1000 meters underground, it transforms into the supercritical state. Furthermore, water in the sub/supercritical state has many specific physical and chemical properties, which can not only provide heat exchange, but also participate in the thermal cracking reaction of oil shale. Therefore, it is necessary to identify the different effects of an anhydrous environment and sub/supercritical water on the pyrolysate characteristics of oil shale and their interaction mechanism.

When water approaches the critical state (T_c = 374.15 °C, P_c = 22.1 MPa), the gas–liquid interface disappears and a homogeneous system is formed, and thus its thermodynamic properties, heat and mass transfer ability and solubility greatly change.[14] Compared with the natural water with ambient temperature and pressure, sub/supercritical water has a lower polarity, lower dielectric constant, weaker hydrogen bonds, and higher ionization constant, and thus can provide more

[a]*Key Laboratory of In situ Property Improving Mining of Ministry of Education, Taiyuan University of Technology, Taiyuan, 030024, China. E-mail: kangzhiqin810101@126.com*

[b]*The In situ Steam Injection Branch of State Center for Research and Development of Oil Shale Exploitation, Taiyuan University of Technology, Taiyuan, 030024, China*

[c]*College of Mining Engineering, Taiyuan University of Technology, Taiyuan, 030024, China*

[d]*Institute of Unconventional Oil and Gas, Northeast Petroleum University, Daqing, 163318, China*

hydronium cations and hydroxide anions and be considered as an acidic and basic catalyst.[15,16] Siskin *et al.* reported that subcritical water is an effective acid–base bicatalyst and its catalytic effect is enhanced by minerals such as clays and carbonates.[17] Also, sub/supercritical water can act as a reactant to induce some unconventional pyrolysis reactions, such as hydrolysis, reforming and methanation reactions, due to its acid–base catalytic effect.[18,19] Further, sub/supercritical water can be used as an efficient heat and mass transfer medium because of its excellent diffusivity and swelling effect, and thus can improve the transfer efficiency.[20,21] Patrick *et al.* reported that the pyrolysis oil remained in the oil shale under high-pressure anhydrous conditions and cracked into hydrocarbon gases, whereas 80% of the pyrolysis oil discharged under high-pressure water conditions and the oil yield also increased.[22] The sub/supercritical water could rapidly bring out shale oil and gas products because of its swelling effect and facilitate the formation of pore channels, reducing the secondary cracking of shale oil. Given that sub/supercritical water can play multiple roles in the conversion of organic matter, such as reactants, catalysts and media, it has remarkable advantages and promising prospects for the exploitation and utilization of oil shale.

In recent years, sub/supercritical water was introduced in extract shale oil and gas from oil shale, and many scholars have increasingly focused on its effect on thermal conversion behavior and hydrocarbon generation from kerogen. Ma *et al.* investigated the hydrous pyrolysis mechanism of Liushuhe oil shale in an autoclave and found that the initial pyrolysis temperature increased by 70 °C and the generation of hydrocarbons became easier in the presence of water.[23] Wang *et al.* selected subcritical water to extract Huadian oil shale under isothermal conditions and determined the optimum reaction conditions. They demonstrated that the atomic H/C of bitumen reached the maximum value when the extraction time was 15 h and macromolecular hydrocarbons cracked into smaller ones, which was attributed to the catalytic process and solvent effect of subcritical water.[24] Lewan *et al.* compared the pyrolysate characteristics of Mahogany oil shale in subcritical water and an anhydrous closed system, = and revealed that subcritical water could extract 29% more hydrocarbons and 33% more C15+ hydrocarbons at 350 °C than the anhydrous system, which is attributed to the dissolution of bitumen in the water and the supply of hydrogen to stabilize the products of thermal cracking, promoting the discharge of immiscible oil.[25] Harfi *et al.* adopted supercritical water to extract Timahdit oil shale and concluded that increasing the extraction temperature could enhance the yields of aromatics and paraffins and reduce the content of asphaltenes.[26] Nasyrova *et al.* studied the effects of subcritical and supercritical water on the generation of hydrocarbons from Domanic shale rocks and showed that the yields of light hydrocarbons (saturated and aromatic hydrocarbons) in the shale oil increased from 33.98% to 39.63% and 48.24%, respectively.[27]

Fushun oil shale is located in Liaoning Province of China, with proven reserves of 4.02 billion tons. The oil shale in this region is characterized by a high ash content, moderate calorific value and low oil content.[28] Thus, it is significant to search for an optimum method to obtain high yield and quality shale oil. In the literature, experiments on the extraction of oil shale with sub/supercritical water for a long time and low temperature environment have been widely reported. However, few studies have focused on the pyrolysate characteristics of Fushun oil shale with sub/supercritical water from low temperature to high temperature and progressively and systematically compared with anhydrous pyrolysis at the corresponding temperature. Therefore, in this work, the pyrolysis experiments of Fushun oil shale in an anhydrous environment, subcritical water and supercritical water were carried out in a simulated *in situ* pyrolysis reactor to investigate their effect on the pyrolysis evolution from 300 °C to 450 °C at high pressure, and the optimum pyrolysis condition was determined. The pyrolysate characteristics in different pyrolysis processes including hydrocarbon gas, discharged/residual oil and solid residuals were compared in detail. In addition, the relationship between sub/supercritical water and hydrocarbon generation and their interaction mechanism were revealed. These results can provide theoretical support and technical guidance for the efficient *in situ* oil shale exploitation with sub/supercritical water.

Material and methods

Sample preparation

The oil shale samples adopted herein were collected from the Fushun mining area in Liaoning Province of China. The color of the oil shale was dark brown, with weak greasy luster, and the rock particles were compact. The Fushun oil shale was crushed and screened into irregular smaller cylindrical samples (diameter of 10 mm and height of 15 mm), and then dried at 110 °C for 24 h. The proximate analysis and ultimate analysis of Fushun oil shale are exhibited in Table 1. As seen in Table 1, the oil shale in this region had a high ash content and moderate volatile content.

Also, the H/C and O/C atomic ratios of its kerogen were 1.38 and 0.11, respectively, indicating that the kerogen type of Fushun oil shale was I-IIa and belonged to immature source rock according to the kerogen-type paradigm diagram of Tissot and Welte, as shown in Fig. 1. Therefore, the Fushun oil shale was in the early stage of the oil generation window and had high oil generation potential.

The prepared samples (each 60 g) were reacted in an autoclave to simulate the *in situ* pyrolysis experiment under various conditions. Then, four samples were selected for anhydrous pyrolysis with the temperature of 300 °C, 360 °C, 450 °C and 500 °C, which were denoted as AN-300, AN-360, AN-450 and AN-

Table 1 Proximate analysis and ultimate analysis of FS oil shale[a]

	Proximate analysis/wad%				Ultimate analysis/wad%				
Sample	M	A	V	FC	C	H	O	N	S_t
FS	3.44	78.08	17.02	1.46	12.57	2.11	11.03	1.09	0.71

[a] ad = air dried.

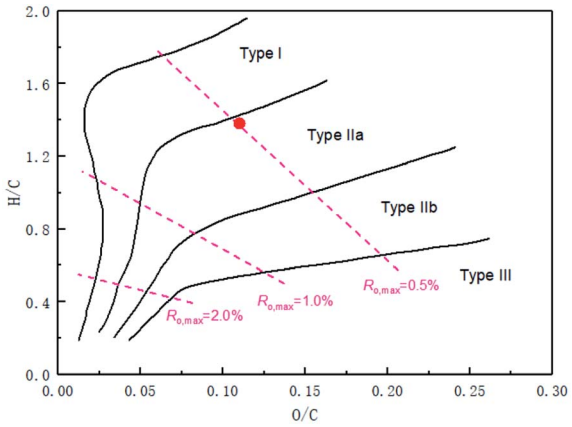

Fig. 1 Kerogen-type paradigm diagram of Tissot and Welte.

500, respectively. Also, two samples were adopted for simulated pyrolysis in subcritical water with the temperatures and pressures of 300 °C and 10 MPa and 360 °C and 20 MPa, which were named SubCW-300 and SubCW-360, respectively. The last sample was used for simulated pyrolysis in supercritical water, and the temperature and pressure were set to 450 °C and 27 MPa, respectively, which was termed SCW-450. All experimental and testing results were on the original dry rock basis.

Pyrolysis equipment

The simulated *in situ* pyrolysis experiments of Fushun oil shale in anhydrous condition and sub/supercritical water were conducted in a DK-III hydrocarbon generation and expulsion system for source rock, simulating the pore-heat-pressure of formation (as shown in Fig. 2). The equipment mainly consisted of five parts including data acquisition system, high temperature and pressure reactor, heating system, cooling and separation system, and product collection system. Before the experiment, the dried samples were loaded into the reactor and the air tightness of the system must be checked.

For anhydrous pyrolysis, the final temperatures were set to 300 °C, 360 °C, 450 °C and 500 °C with the heating rate of 1 °C min^{-1}. Also, the pyrolysis experiments were maintained for 48 h at the final temperatures to ensure the complete pyrolysis of organic matter and expulsion of oil and gas. Also, the generated hydrocarbons were all discharged from the reactor after the pyrolysis was completed.

For sub/supercritical water pyrolysis, the final temperatures were set to 300 °C, 360 °C and 450 °C, and the corresponding pressures were controlled as 10, 20 and 27 MPa. The heating rate was also 1 °C min^{-1}. Also, 15–45 mL water was loaded into the reactor to produce the set pressure obtained from the expansion of steam and the generation of hydrocarbons during pyrolysis. When the pressure of the system reached the set value, the generated hydrocarbons were discharged from the reactor to maintain the specified pressure. This process was cycled and maintained for 48 h under the final conditions to ensure the complete pyrolysis of organic matter and expulsion of oil and gas.

After complete pyrolysis, dichloromethane was used to flush the pipeline and reactor when the pyrolysis system cooled to 180 °C. The oil in the cold hydrazine Dewar bottle was called discharged oil I and the oil in the pipeline was called discharge oil II. The sum of discharged oil I and II was called total discharged oil. The oil extracted from the residual solid was called residual oil. Finally, the components of oil and gas were identified by gas chromatography and the residual solids after extraction were weighed and analysed *via* a Rock-Eval pyrolysis experiment.

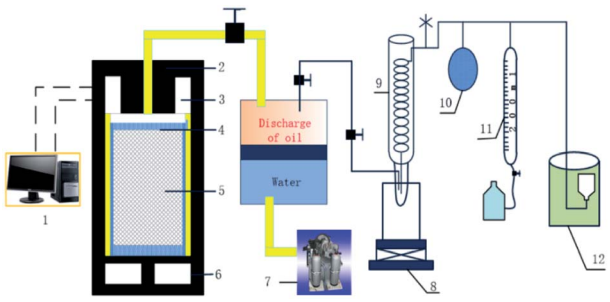

Fig. 2 Schematic diagram of anhydrous and sub/supercritical water pyrolysis experiment, where 1-computer, 2-heating system, 3-parallel block, 4-filter block, 5-oil shale sample, 6-sealing plunger, 7-high pressure balance pump, 8-cold hydrazine Dewar bottle, 9-condenser, 10-buffer airbags, 11-gas volume measurer, and 12-gas collector.

Characterization of pyrolysis products

The component of pyrolysis gas was detected using a GC-950 and GC 9890A. The GC-950 had two TCDs and two channels. Its carrier gas was H_2 with a flow rate of 40 mL min^{-1}. The yields of CH_4 and CO in pyrolysis gas were tested using a 5A molecular sieve column, while the yields of CO_2 and C_2–C_4 hydrocarbons in the pyrolysis gas were determined using a GDDX-502 column. In addition, the H_2 in the pyrolysis gas was analyzed using a 5A molecular sieve column in the GC 9890A. Its carrier gas was N_2 with a flow rate of 40 mL min^{-1}.

The discharged and residual oil obtained from the pyrolysis experiments were diluted with toluene and tested using an Agilent 7890 GC with an online injector and 5795N mass spectrum (MS) detector. For GC, the column was an HP-5MS (30 m × 0.25 mm × 0.25 μm) fused silica capillary column. Also, the carrier gas was helium with the flow rate of 1 mL min^{-1}. The injection temperature was 280 °C, and the temperature programme was 3 min at 50 °C, and then heated to 300 °C at the heating rate of 5 °C min^{-1} and maintained for 5 min at the final temperature. For MS, the ionization energy was 70 eV and mass scanning range 40–400 amu. The electron impact source was EI.

The SARS group component analysis was conducted to identify the fraction of saturates, aromatics, resins and asphaltenes by column chromatography. Briefly, aluminum oxide was adopted as the column chromatography medium to separate the saturates with *n*-heptane, aromatics with toluene, resins with toluene and methanol (1 : 1), and the asphaltenes were removed by centrifuging at the beginning because of their insolubility in *n*-heptane. Trichloroethylene was employed to

rinse the aluminum oxide off the remaining residue. The percentage of saturates was calculated by difference due to the high volatility when separating the saturates and solvents by boiling them.

The geochemical characteristic of the residual solid product was determined using a Rock-Eval 6 rock pyrolysis analysis instrument. The parameters of S_1, S_2, S_3 and T_{max} were determined, and the hydrogen index (HI) was calculated accordingly. The temperature for maximum hydrocarbon generation (T_{max}) was defined based on the maximum value of the S_2 peak, which was regarded as a maturity indicator.

Results and discussion

The mass loss of oil shale in different pyrolysis conditions

The relation between mass loss and temperature of Fushun oil shale during anhydrous pyrolysis, subcritical and supercritical water pyrolysis is shown in Fig. 3. It can be seen that the mass loss of the oil shale samples was enhanced with an increase in temperature due to the thermal cracking of organic matter, which was quite different in the various pyrolysis modes. During anhydrous pyrolysis, the mass loss rapidly increased at 300–450 °C and much more slowly at 450–500 °C, indicating that the thermal degradation of organic matter was mostly completed at 450–500 °C. The maximum mass loss of oil shale was 11.37% at the temperature of 500 °C. By contrast, during subcritical and supercritical water pyrolysis, the mass loss rates of oil shale were significantly higher than that during anhydrous pyrolysis, which suggests that subcritical and supercritical water was beneficial for the pyrolysis of organic matter and promoted the release of volatile oil and gas. The subcritical and supercritical water had little influence on the pyrolysis of oil shale at the temperature of 300 °C, which was attributed to the fact that the kerogen had not begun to be significantly cracked, but firstly converted to asphaltenes, accompanied by the release of small molecular gases at this temperature.[29,30] When the pyrolysis system reached the states of S_{ub}CW-360 and SCW-450, the sub/supercritical water had an acid–base catalysis and swelling effect, which could participate in the cracking of kerogen and facilitate the pyrolysis reaction, resulting in a decrease in the yield of the solid residuals.[15,16] The mass loss rate of oil shale reached the highest value (12.30%) at the temperature of 450 °C and pressure of 27 MPa, which was even higher than that during anhydrous pyrolysis at 500 °C. Thus, sub/supercritical water exhibited significant advantages in the pyrolysis of oil shale and promoted the formation and release of the oil and gas.

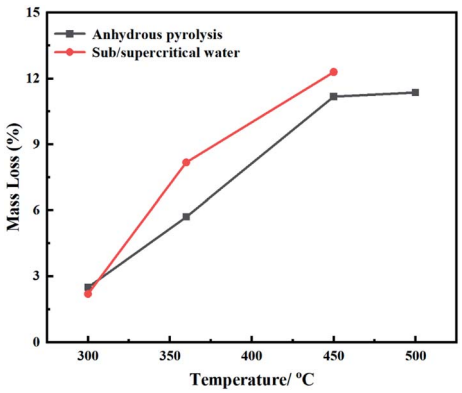

Fig. 3 Mass loss of oil shale in anhydrous pyrolysis and sub/supercritical water pyrolysis.

The yields of pyrolysis products

Fig. 4 displays the pyrolysate yields of Fushun oil shale in anhydrous pyrolysis, subcritical and supercritical water pyrolysis. As shown in Fig. 5(a), the yield of pyrolysis gas of oil shale in different pyrolysis modes enhanced with the increase of temperature. At the temperatures of 300 °C and 360 °C during anhydrous pyrolysis, only a small amount of gas was released, which included some adsorbed gas and micromolecule gas, due to the insufficient cracking of kerogen at low temperature.[31] When the pyrolysis temperature reached 450 °C, the aliphatic

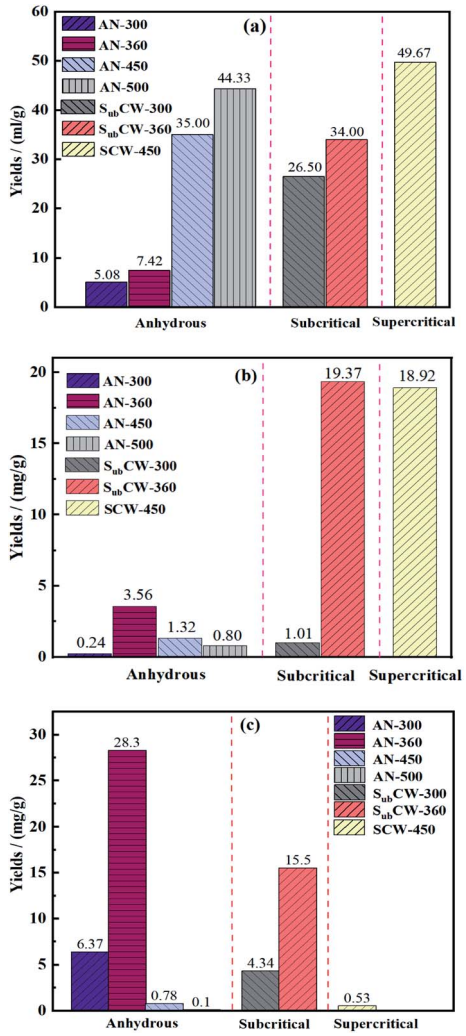

Fig. 4 Yields of pyrolysates in anhydrous pyrolysis, subcritical and supercritical water pyrolysis (a, pyrolysis gas, b, discharged oil, and c, residual oil).

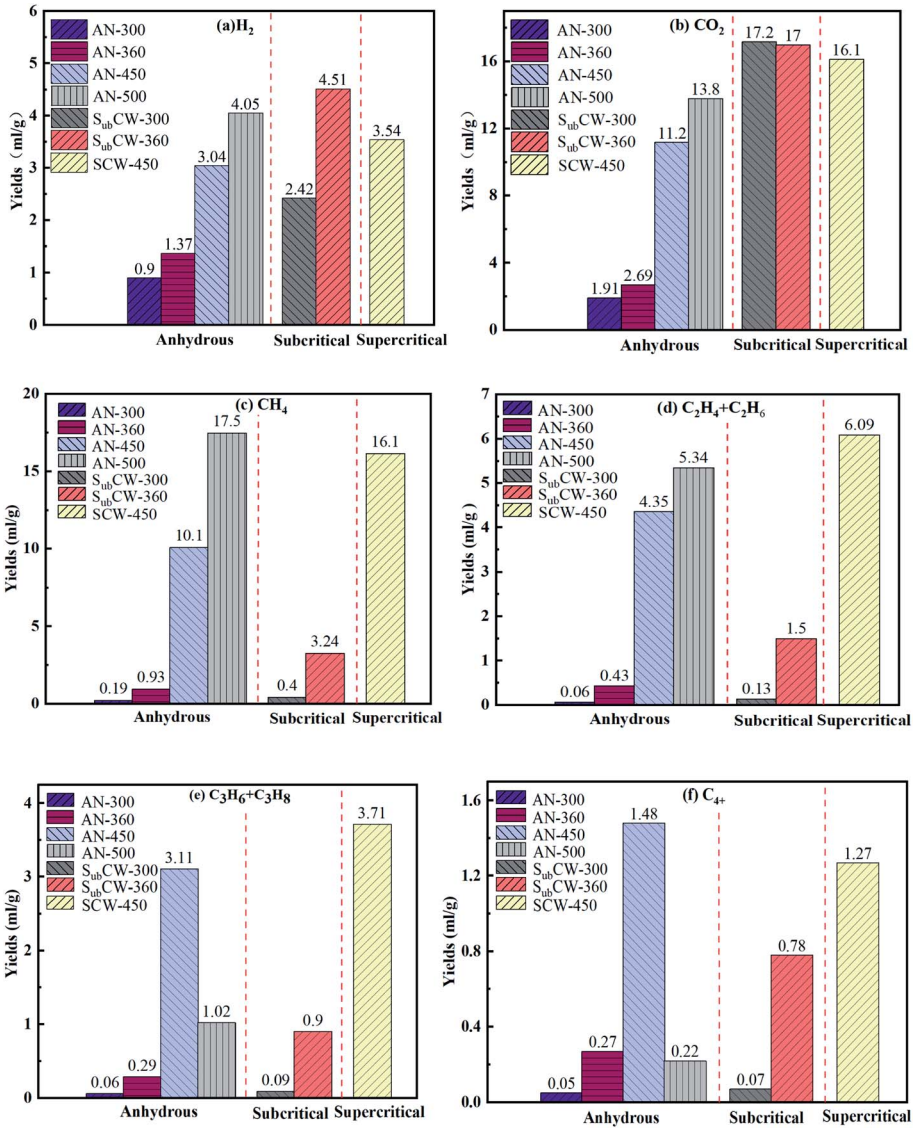

Fig. 5 Gas composition collected from the pyrolysis of FS oil shale under three conditions. (a) H_2, (b) CO_2, (c) CH_4, (d) C_2H_4 + C_2H_6, (e) C_3H_6 + C_3H_8, (f) C_{4+}.

chains and aromatic side chains of kerogen sequentially cracked, resulting in the release of pyrolysis gas in major quantities.[32] When the final temperature was set to 500 °C, the yield of pyrolysis gas reached 44.33 mL g^{-1}. Furthermore, in subcritical and supercritical water pyrolysis, the yields of pyrolysis gas were higher than that at the corresponding temperature compared with anhydrous pyrolysis. At the temperature of 300 °C and pressure of 10 MPa, it is worth noting that the yield of pyrolysis gas reached 26.5 mL g^{-1}, which was 5.22 times that during anhydrous pyrolysis. The subcritical and supercritical water had strong extraction ability and promoted the formation and release of small molecule gas.[23] When the pyrolysis system was in the supercritical state (SCW-450), the yield of pyrolysis gas was 49.67 mL g^{-1}, which was even higher than that at the temperature of 500 °C during anhydrous pyrolysis. Therefore, subcritical and supercritical water can facilitate the generation of gas product from oil shale during pyrolysis.

As exhibited in Fig. 4(b), the yields of discharged oil from Fushun oil shale in anhydrous pyrolysis first increased, and then decreased with an increase in temperature. The macromolecule structure of kerogen began to crack when the temperature increased. Also, the unstable bridge bonds in the kerogen broke and a large amount of free radicals was released.[33] The free radicals combined to form shale oil, and the yield of discharged oil increased. The maximum yield of discharged oil was 3.56 mg g^{-1} at the temperature of 360 °C. When the pyrolysis temperature reached 450 °C and 500 °C, the shale oil underwent a secondary pyrolysis reaction and cracked into gaseous hydrocarbons in the semi-closed system, leading to a decrease in the discharged oil and significant increase in pyrolysis gas.[34] In addition, in anhydrous pyrolysis, the yields of discharged oil were in minor quantities, which is consistent with the result by Patrick.[22] The permeability of the oil shale sample was relatively low at high pressure under anhydrous

conditions, leading to limited seepage channels, and thus weak migration capacity of shale oil.[35] Thus, the shale oil was hardly discharged during anhydrous pyrolysis and a secondary cracking reaction also occurred.

By contrast, the effect of subcritical and supercritical water on the yields of discharge oil during pyrolysis was obviously significant at high temperature. When the pyrolysis temperature was 300 °C and the pressure was 10 MPa, the yield of discharged oil was also in minor quantities due to the low temperature. When the pyrolysis system reached the subcritical condition of SubCW-360, the yield of discharged oil sharply increased by 5.44 times that in anhydrous pyrolysis. Furthermore, When the pyrolysis system reached the supercritical condition of SCW-450, the yield of discharged oil slightly decreased, owing to the increase in gas yield as a result of secondary cracking reactions, but was 14.3-times that in anhydrous pyrolysis at the same temperature. This is because sub/supercritical water had a high ion product constant and could provide more hydrogen ions, which could promote acid-catalysed carbocation reactions, resulting in the formation of organic acids. Subsequently, these organic acids act as transfer agents for hydride ions and avoid the polymerization into shale char, promoting the generation of shale oil. Simultaneously, sub/supercritical water could act as a diffusion medium because of its strong swelling effect, which was conducive to extracting and carrying the shale oil accumulated in the pores and channels of oil shale and reducing its viscosity.[36] Thus, the subcritical and supercritical water had a positive role in the production of shale oil. The maximum yield of discharged oil occurred under the condition of SubCW-360 rather than SCW-450, which was 19.37 mg g^{-1}.

As seen in Fig. 4(c), whether in anhydrous or hydrous pyrolysis, the yields of residual oil exhibited a trend of increasing initially, and then decreasing as the temperature increased. In anhydrous pyrolysis, the yield of residual oil reached the maximum at the temperature of 360 °C, which was mainly attributed to the fact that the kerogen cracked into volatile oil and gas, but hardly discharged in time at this temperature in the high-pressured semi-closed system. Therefore, a large amount of shale oil remained in the pores and channels of the residual solid. When the pyrolysis temperature reached 450 °C and 500 °C, there was a small amount of residual oil in the residual solid, but a large amount of pyrolysis gas was generated, which is due to the fact that the shale oil remaining in the residual solid cracked into micromolecule gas in the pores and channels and released. While, in subcritical and supercritical water pyrolysis, the yields of residual oil were lower than that in anhydrous pyrolysis. According to Fig. 4(a)–(c), the supercritical water could extract the most oil and gas in the oil shale, and there was extremely less residual oil in the residual solid, which was 0.53 mg g^{-1} (in SCW-450). The sub/supercritical water with a higher diffusion coefficient and lower viscosity had driving and swelling effects during pyrolysis of oil shale.[37] These effects could make the phase interface disappear and reduce the interfacial tension, thereby reducing the viscosity and improving the fluidity of the oil. Also, the generated oil was dissolved in sub/supercritical water to form a miscible phase due to their strong solubility and easily migrated to the outside.[38] Simultaneously, the generated CO_2 was also in the supercritical state under this condition, and it also had driving and swelling effects, but their ability was weaker than that in sub/supercritical water.[39,40] Consequently, it could be obviously seen that the subcritical and supercritical water had an advanced effect on the generation, migration and release of volatile oil and gas during pyrolysis because of their special properties.

Analysis of pyrolysis gas

Fig. 5 displays the gas composition of Fushun oil shale at different final temperatures collected from anhydrous, subcritical and supercritical water pyrolysis. As shown in Fig. 5(a), during anhydrous pyrolysis, the yield of H_2 continued to rise as the final temperature increased because the C–H bond cracked and more hydrogen radicals were generated during pyrolysis, which combined to form H_2. Also, the H_2 produced by the pyrolysis of FS oil shale was derived from the dehydrogenation of aromatic rings, the cyclization of aliphatic alkanes, and the aromatization of naphthenes at low temperatures, and mainly from the polycondensation reactions of aromatic structures and heterocyclic compounds and water–gas shift reaction at high temperatures.[41] Thus, there was a small amount of H_2 before 360 °C, which was less than 1.5 mL g^{-1}. When the pyrolysis temperature was 500 °C, the yield of H_2 was the maximum and reached 4.05 mL g^{-1}. While, in sub/supercritical water pyrolysis, the yields of H_2 also exhibited an increasing trend initially, and then decreasing trend, which were higher than that during anhydrous pyrolysis at the corresponding temperature. Especially, the yield of H_2 under the condition of SubCW-360 was 3.29 times that under the condition of AN-360, which reached the maximum value of 4.51 mL g^{-1} and even higher than that under the condition of AN-500. The main reason for this was that the water–gas shift reaction ($CO + H_2O \rightarrow CO_2 + H_2$) occurred in the presence of sub/supercritical water during the pyrolysis of oil shale and sub/supercritical water provided a large amount of hydrogen source, which led to an improvement in the production of H_2.[42] Simultaneously, the results of gas chromatography revealed that CO was not detected at different temperatures, which is because CO was consumed by a large amount of sub/supercritical water to produce H_2. When the pyrolysis system reached the supercritical state, the water–gas shift reaction was inclined to proceed in the reverse direction due to the higher temperature, which resulted in a decrease in the H_2 yield.

As presented in Fig. 5(b), during anhydrous pyrolysis, the yield of CO_2 continued to increase with an increase in temperature. Before the pyrolysis temperature of 360 °C, a small amount of physically adsorbed CO_2 in the oil shale escaped. When the pyrolysis temperature further increased, the carboxyl and ester groups in kerogen began to crack, and thus decarboxylation and hydrolysis reactions occurred, forming CO_2.[43] The yield of CO_2 reached the maximum value at the temperature of 500 °C, which was 13.8 mL g^{-1}. In contrast, under the effect of subcritical and supercritical water, the CO_2 yields of oil shale

slightly decreased as the pyrolysis temperature increased, which were higher than that during anhydrous pyrolysis. There were three reasons for this phenomenon, where the first is that some CO_2 during the sub/supercritical water pyrolysis of oil shale originated from the water–gas shift reaction, the second was that sub/supercritical water facilitated the process of decarboxylation reaction, and the third was that sub/supercritical water, as an acid–base catalyst, catalyzed the hydrolysis of ester to produce carboxylic acid and alcohol.[16] Also, sub/supercritical water could promote the decomposition of carboxylic acid and alcohol into CO_2. Furthermore, compared with the supercritical water condition, the hydrolysis of ester occurred more easily in subcritical water.[44]

As exhibited in Fig. 5(c), the yields of CH_4 generally increased as the pyrolysis temperature rose during anhydrous pyrolysis and sub/supercritical water pyrolysis. The released CH_4 in the pyrolysis gas was derived from low-temperature desorption and hydrogenation of methyl and methoxy groups on the aromatic rings and aliphatic chains.[45] Thus, the yield of CH_4 before the temperature of 360 °C was in minor quantities because it originated from the physically adsorbed gas in the oil shale pores. When the pyrolysis temperature reached 450 °C, the methyl and methoxy in kerogen began to crack and a large amount of CH_4 was generated. Thus, the yield of CH_4 reached the maximum value at the temperature of 500 °C, which was 17.5 mL g^{-1} during anhydrous pyrolysis. While, during sub/supercritical water pyrolysis, it was found that the yields of CH_4 were higher than that during anhydrous pyrolysis at the same temperature. This is because sub/supercritical water had the activity of promoting the cracking of methyl and methoxy side chains and enhanced the yield of CH_4, which was ascribed to the fact that sub/supercritical water could provide more hydrogen source and acid–base catalytic effect. Meanwhile, as the pyrolysis temperature increased, the secondary reaction of volatile hydrocarbons in half-closed system intensified, which resulted in an improvement in the CH_4 yield.

As shown in Fig. 5(d), the total yields of C_2H_4 and C_2H_6 in the pyrolysis gas of FS oil shale continuously rose with an increase in temperature during both anhydrous pyrolysis and sub/supercritical water pyrolysis. The total yields of C_2H_4 and C_2H_6 of FS oil shale during sub/supercritical water pyrolysis were higher than that during anhydrous pyrolysis. The C_2H_4 and C_2H_6 yields were low below 360 °C, and then rose sharply when the pyrolysis temperature reached 450 °C. Also, the concentration of total C_2H_4 and C_2H_6 at the temperature of 360 °C during subcritical water pyrolysis was 3.49 times that in anhydrous pyrolysis, which indicates that the subcritical water could promote the release of C_2H_4 and C_2H_6. Furthermore, the concentration of total C_2H_4 and C_2H_6 at the temperature of 450 °C during subcritical water pyrolysis was even higher than that at the temperature of 500 °C during anhydrous pyrolysis, which was the maximum value of 6.09 mL g^{-1}. The C_2H_4 and C_2H_6 in the pyrolysis gas of oil shale originated from the alkyl radicals in kerogen losing or receiving a hydrogen free radical. The presence of sub/supercritical water could improve the breaking of the aliphatic hydrocarbon and aromatic ring side chains or secondary cracking reaction. Also, relevant literature showed that in the atmospheres of CH_4–CO_2 at high temperature and CO–H_2O in the sub/supercritical state, more $^{\cdot}H$ free radicals could be provided, which resulted in an improvement in the C_2H_4 and C_2H_6 yield.[46,47]

The yields of aliphatic hydrocarbons included C_3 and C_{4+} in the pyrolysis gas, as shown in Fig. 5(e) and (f), respectively, which exhibited an increasing trend initially, and then decreasing trend during anhydrous pyrolysis, and a continuous upward trend during sub/supercritical water pyrolysis. This is because a higher pyrolysis temperature induced the cracking of the long-chain aliphatic hydrocarbon and aromatic ring side chains, while a further increase in temperature exceeding 450 °C led to the cleavage of C_3 and C_{4+} into short-chain hydrocarbons, *e.g.*, propane could crack into methane and ethylene at 500 °C.[48] Therefore, the yields of aliphatic hydrocarbons C_3 and C_{4+} reached the maximum values at the temperature of 450 °C. Also, the sub/supercritical water facilitated the release of the aliphatic hydrocarbons of C_3 and C_{4+} at a lower temperature. Furthermore, the yields of C_3 and C_{4+} in the pyrolysis gas of oil shale during sub/supercritical water pyrolysis were higher than that during anhydrous pyrolysis except for the yield of C_{4+} at the temperature of 450 °C. Thus, the yields of C_3 and C_{4+} during sub/supercritical water pyrolysis were 3.10 and 2.89 times than that during anhydrous pyrolysis at the temperature of 360 °C, respectively. This is attributed the fact that sub/supercritical water has ability of promoting the cleavage of aliphatic hydrocarbon and aromatic ring side chains due to their solvent effect and provides more $^{\cdot}H$ free radicals and CH_4–CO_2 and CO–H_2O atmosphere, reducing the bond energy of C–H/C–H. Also, under the effect of supercritical water, the aliphatic hydrocarbons of C_{4+} were inclined to crack into short-chain ones, resulting in a lower amount than that during anhydrous pyrolysis.

Analysis of shale oil

The component of discharged oil. The group components of the discharged oil from anhydrous pyrolysis and sub/

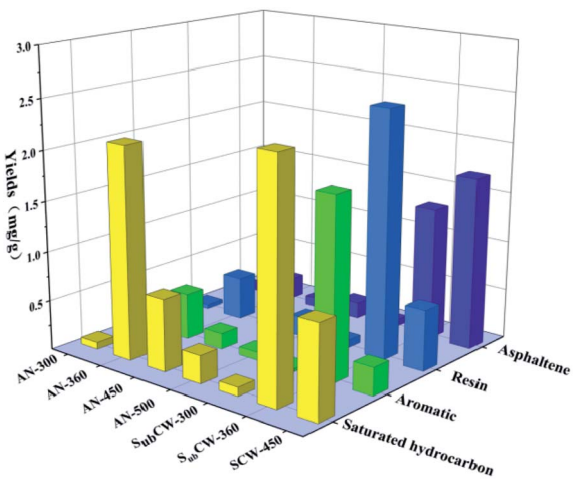

Fig. 6 Components of discharged oil from anhydrous pyrolysis and sub/supercritical water pyrolysis.

Table 2 The component distribution of discharged oil from two pyrolysis modes

Pyrolysis mode/%	Saturated hydrocarbon	Aromatic	Resin	Asphaltene
AN-300	50.08	13.69	24.64	11.60
AN-360	65.43	14.31	13.35	6.91
AN-450	60.08	13.54	18.87	7.51
AN-500	49.07	10.89	23.17	16.86
S_{ub}CW-300	32.20	12.89	29.54	25.37
S_{ub}CW-360	29.36	22.81	31.07	16.75
SCW-450	26.20	8.02	19.11	46.66

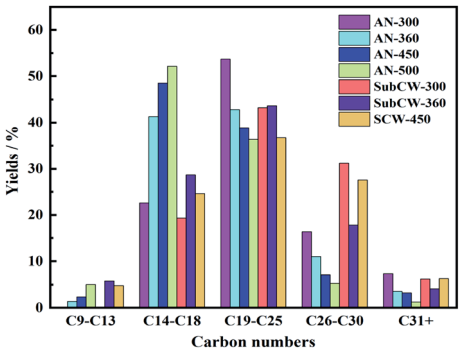

Fig. 7 Carbon number distribution of discharged oil from two pyrolysis modes.

supercritical water pyrolysis of FS oil shale were obtained, as shown in Fig. 6 and Table 2. The discharged oil was divided into four parts, including saturated hydrocarbons, aromatics, resins and asphaltenes. As displayed in Fig. 7, the yields of saturated hydrocarbons, aromatics, resins and asphaltenes exhibited firstly and increasing, and then decreasing trend with an increase in temperature during anhydrous pyrolysis, and they all reached the maximum values at the temperature of 360 °C, which is consistent with the yield of the discharged oil. Consequently, the proportions of saturated hydrocarbons and aromatics were the highest and the fractions of resins and asphaltenes were the lowest at this temperature, as seen in Table 2. This is attributed to the fact that some saturated hydrocarbons and aromatics cracked into small molecule gas with an increase in temperature, reducing their proportions in the discharged oil.

Furthermore, the yields of saturated hydrocarbons, aromatics and resins displayed firstly an increasing, and then decreasing trend as the temperature increased during sub/supercritical pyrolysis, but the asphaltenes yield continued to increase. The contents of the four components in the shale oil from sub/supercritical water pyrolysis were higher than that from anhydrous pyrolysis at the same temperature. The reason for this is that the oil shale was pyrolyzed in a hydrogen-rich environment, and the alkyl and aromatic hydrocarbons could readily combine with the hydrogen source to form saturated and aromatic hydrocarbons, which inhibited the polymerization of the coking reaction. Also, the component of shale oil was dominated by saturated hydrocarbons in anhydrous pyrolysis, which accounted for 50–65% of the total oil. While, during sub/supercritical water pyrolysis, a large amount of resins and asphaltenes formed in the shale oil, especially in the supercritical water state. This is because sub/supercritical water has dissolving capacity, and thus could directly extract the resin and asphaltene macromolecules from the kerogen. The organic matter in the oil shale was inter-crosslinked with inherent minerals through chemical bonds and the organic matter was adsorbed on the inherent mineral surface. The oxygen-containing bonds in the resin and asphaltene were combined on the inherent minerals in the form of coordination bonds and ionic bonds.[49] The presence of sub/supercritical water could weaken the adsorption of organic matter on the inherent minerals, reduce their bond energy, and generate a large amount of macromolecule resin and asphaltenes due to the weak thermal cracking. Also, the sub/supercritical water could induce acid-catalysed carbocation reactions and cleave the ether and ester bonds, which depolymerized the macromolecule kerogen, resulting in an enhancement in the resin and asphaltene yield.[14] When the pyrolysis temperature increased from 360 °C to 450 °C, the resins could transform into asphaltenes by condensation reaction due to their weak thermal stability.[50] Under the condition of SCW-450 °C, the content of resin and asphaltene in the shale oil reached the highest, which accounted for 65.77%.

According to their carbon number, the components of the discharged oil were further classified as five parts to deeply compare the influence of the anhydrous environment and sub/supercritical water on the chemical composition of the discharged oil. As illustrated in Fig. 7, the distribution of carbon numbers (from short-chain to long-chain) exhibited first an increasing, and then decreasing trend, and the diesel (C14–C18) and lubricant (C19–C25) were dominant in the discharged oil in both pyrolysis modes. During anhydrous pyrolysis, the contents of light fractions (C9–C13) and medium fractions (C14–C18) were enhanced, and the heavy fractions (C19+) declined with an increase in temperature. The heavy oil firstly precipitated at low temperature, and then light oil released because of sufficient cracking as the temperature increased. Also, at 300 °C during anhydrous and subcritical pyrolysis, the presence of light fractions (C9–C13) was not detected. Thus, the discharged oil at high temperature was lighter than that at low temperature in anhydrous pyrolysis. While, during sub/supercritical water pyrolysis, the contents of light fractions (C9–C13) and medium fractions (C14–C18) and heavy fractions (C19–C25) increased first, and then decreased with an increase in temperature, while

the heavy fractions (C26–C30 and C30+) exhibited the opposite trend. Thus, the discharged oil under the condition of S_{ub}CW-360 was lighter than that of S_{ub}CW-300 due to its higher temperature. Also, the discharged oil during supercritical water pyrolysis was heavier than that during subcritical water pyrolysis. Generally, sub/supercritical water could enhance the yields of discharged oil, while the discharged oil obtained from sub/supercritical water pyrolysis was heavier than that from anhydrous pyrolysis. This result is consistent with the group component analysis of the discharged oil, which contained a large amount of resin and asphaltene with higher carbon numbers due to the solvent effect. Also, the ionic product and solvating power of supercritical water are less than that of subcritical water. Thus, the discharged oil from subcritical water pyrolysis had a higher quantity and lighter quality than that from supercritical water pyrolysis.

The component of residual oil. The yields and mass fractions of the four components in the residual oil during anhydrous pyrolysis and sub/supercritical water pyrolysis of FS oil shale are displayed in Fig. 8 and Table 3. As seen in Fig. 8 and Table 3, the heavy components of resins and asphaltenes with high boiling points were dominant in the residual oil. The yields of the four components in the residual oil exhibited first an increasing, and then decreasing trend, and reached the maximum values at the temperature of 360 °C, which is consistent with the yields of residual oil. Also, when the temperature reached 450 °C, the amount of the four components was in minor quantities, which was less than 1 mg g^{-1}. This is attributed to the fact that a higher temperature significantly promoted the release and migration of shale oil. Furthermore, the mass fractions of saturated and aromatic hydrocarbons continuously increased as the temperature increased, while the mass fractions of resins and asphaltenes exhibited the opposite trend in the two pyrolysis modes. This is because a higher temperature induced the deeper cracking of resins and asphaltenes. In the two pyrolysis modes, the amounts of resins and asphaltenes were much higher than saturated and aromatic hydrocarbons in the residual oil. Therefore, the heavy components of resins and asphaltenes easily remained in the residual oil. This is because the resins and asphaltenes were released less readily from the pores and channels in the oil shale, which was due to their high viscosity and weak migration capacity. Also, the sub/supercritical water could extract macromolecule fragments in kerogen at a lower temperature and form resins and asphaltenes due to the solvent effect. Thus, according to Table 3, the mass fractions of resins and asphaltenes of the residual oil from sub/supercritical water pyrolysis were higher than that from anhydrous pyrolysis at the same temperature.

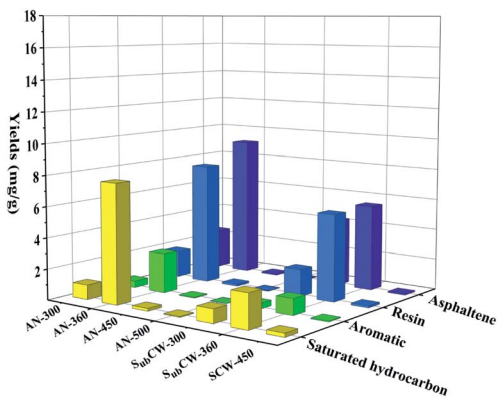

Fig. 8 Components of residual oil in anhydrous pyrolysis and sub/supercritical water pyrolysis.

As illustrated in Fig. 9, the carbon number distribution (from short-chain to long-chain) of the residual oil of each sample increased initially, and then decreased during anhydrous pyrolysis and sub/supercritical water pyrolysis. Also, the light fractions (C9–C13) in the residual oil disappeared and were released from the pores and channels of oil shale due to their low viscosity and strong migration capacity, and thus the heavy fractions (C19+) were dominant in the residual oil. In both pyrolysis modes, the carbon number distribution of residual oil exhibited a fluctuating trend with an increase in temperature. While, the variation trend of the medium fractions (C14–C18) was opposite to that of the heavy fractions (C26–C30), and the variation trend of heavy fractions (C19–C25) was opposite to that of the heavy fractions (C31+) in the two pyrolysis modes. Thus, the heavy fractions (C26–C30) of residual oil may crack into the lighter fractions (C14–C18), and the heavy fractions (C31+) may break into lighter fractions (C19–C25) as the temperature increased. Consequently, the heavy fractions in the residual oil during sub/supercritical water pyrolysis were higher than that during anhydrous pyrolysis because of the presence of resin and asphaltenes.

Analysis of solid residue

The solid residues of FS oil shale after anhydrous pyrolysis and sub/supercritical water pyrolysis were analyzed using Rock-Eval

Table 3 The component distribution of residual oil in two pyrolysis modes

Pyrolysis mode/%	Saturated hydrocarbon	Aromatic	Resin	Asphaltene
AN-300	16.63	7.52	30.75	45.10
AN-360	28.27	9.42	28.80	33.51
AN-450	39.87	11.39	27.75	20.99
AN-500	48.80	13.20	26.20	11.80
S_{ub}CW-300	12.23	4.96	34.94	47.87
S_{ub}CW-360	24.37	7.30	32.79	35.54
SCW-450	34.88	10.11	29.28	25.73

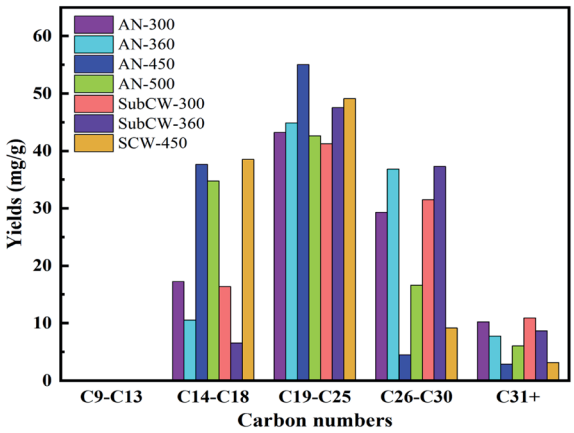

Fig. 9 Carbon number distribution of residual oil in two pyrolysis modes.

pyrolysis equipment, and the geochemical characteristics are exhibited in Fig. 10. As shown in Fig. 10, the total organic carbon content (TOC) of the solid residuals from anhydrous pyrolysis and sub/supercritical water pyrolysis were more than 6% and 4%, respectively. Also, the TOC of the original oil shale was 7.9% according to previous work, and thus a large proportion of organic carbon remained in the oil shale in both pyrolysis modes. Also, the parameters of TOC content and pyrolysable carbon content (PC) decreased with an increase in temperature, indicating that the organic matter of solid residuals decreased. This is because the organic matter in kerogen gradually cracked and depolymerized as the temperature rose. While, the TOC and PC contents of the solid residuals from sub/supercritical water pyrolysis were lower than that from anhydrous pyrolysis at the same temperature, which was attributed to the fact that sub/supercritical water could improve the conversion of organic matter into oil and gas. Also, the declining rates of TOC and PC contents with an increase in temperature during sub/supercritical water pyrolysis were higher than that during anhydrous pyrolysis. The lowest TOC and PC contents of the solid residuals were from supercritical water pyrolysis at 450 °C, which were 4.38% and 0.11%, respectively. Thus, the supercritical water had the strongest influence on the conversion of organic carbon in kerogen during pyrolysis.

The hydrocarbon generation potential (S1 + S2) of solid residuals followed a decreasing trend with an increase in temperature. The S1 + S2 content of the original FS oil shale was 51.95 mg g^{-1} rock, suggesting a superior hydrocarbon generation potential. When the pyrolysis temperatures were 300 °C and 360 °C, the S1 + S2 contents of the solid residuals still exceeded 10 mg g^{-1} rock in the two pyrolysis modes, and thus a large proportion of generated hydrocarbons remained in the oil shale at this temperature. When the pyrolysis temperature reached 450 °C, the S1 + S2 contents of the solid residuals were less than 1 mg g^{-1} rock, indicating that most of the hydrocarbons in the kerogen was released. While, the solid residuals from sub/supercritical water pyrolysis contained less S1 + S2 contents than that from anhydrous pyrolysis, which was due to the fact that the sub/supercritical water could promote the cracking of kerogen to form more hydrocarbons. The lowest S1 + S2 content of solid residual existed in the condition of SCW-450, which was 0.72 mg g^{-1} rock. Accordingly, the supercritical water had the best effect on the release and migration of generated hydrocarbons during the pyrolysis of oil shale, resulting in the least hydrocarbons in the solid residuals.

In addition, the hydrogen index (HI = S2/TOC) also declined as the temperature increased, which is also another index of kerogen type and hydrocarbon generation potential.[51] The HI index of the original FS oil shale was 647.5 mg g^{-1}, and thus the kerogen of FS oil shale was type I. Also, at the temperature of 300 °C during anhydrous pyrolysis and subcritical water pyrolysis, the HI indices of the solid residuals were 530 and 445 mg g^{-1}, respectively, indicating that the solid residuals were still fair source rock with II1 type kerogen. This is because less organic matter in kerogen cracked at low temperature. When

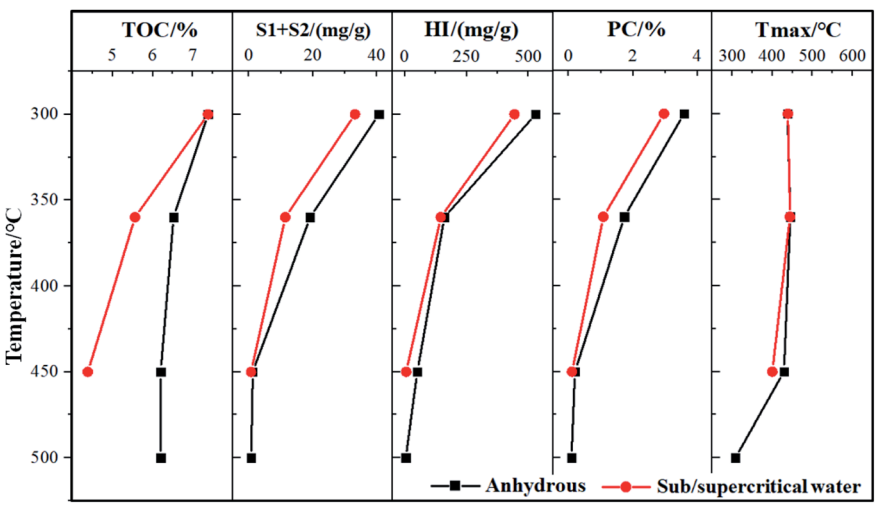

Fig. 10 Geochemical characteristics of solid residues in two different pyrolysis modes.

the temperature reached 360 °C in the two pyrolysis modes, the HI indices of the solid residuals decreased to 130–145 mg g^{-1}. Thus, the kerogen of the solid residuals had evolved into type III, which mainly produced hydrocarbon gas. Also, the most shale oil was formed and released from oil shale at the temperature of 360 °C in two pyrolysis modes, which was consistent with the yield of shale oil in Section 3.2. Furthermore, as the pyrolysis temperature exceeded 450 °C, the HI indices of the solid residuals were reduced to less than 20 mg g^{-1}. The hydrocarbon generation potential of kerogen decreased to the minimum level, which was due to the fact that most of the kerogen was converted into oil and gas and released. While, the HI indices of the solid residuals from sub/supercritical water pyrolysis were lower than that from anhydrous pyrolysis at the same temperature, which demonstrates that sub/supercritical water facilitated the formation and release of oil and gas during pyrolysis due to the solvent effect and thermal cracking. The lowest HI index existed in the condition of SCW-450, and thus the supercritical water had superior ability for the extraction of hydrocarbons compared to subcritical water.

The index of T_{max} indicates the thermal maturity status of the source rock,[52] which exhibited first an increasing, and then decreasing trend with an increase in temperature during anhydrous pyrolysis and sub/supercritical water pyrolysis. The T_{max} index of the solid residuals was 438–445 °C in two the pyrolysis modes at the temperature of 300 °C and 360 °C. Thus, the solid residuals in these pyrolysis modes were still in the stage of oil generation, given that most of the potential oil and gas in the kerogen of oil shale had not yet been generated and released at these temperatures. Also, the subcritical water had little effect on the T_{max} of the solid residuals at the temperature of 300 °C and 360 °C. When the temperature further increased, the T_{max} of the solid residuals in two pyrolysis modes was lower than 450 °C, suggesting that they were in the immature status. Also, there was little hydrocarbon remaining in the solid residuals at high temperatures. Furthermore, the supercritical water reduced the T_{max} value of the solid residual compared with that from anhydrous pyrolysis at the same temperature, resulting in the lower maturity of the solid residual.

Discussions

The pyrolysis mechanism of oil shale is affected by many factors, such as operating condition, pyrolysis atmosphere and heating method. The above-mentioned experimental results and analysis revealed that the pyrolysis behavior of oil shale in a sub/supercritical water atmosphere is controlled by multiple mechanisms, including a series of physical effects and chemical reactions, as shown in the schematic diagram in Fig. 11. According to the above-mentioned results, sub/supercritical water could enhance the yield of oil and gas during the pyrolysis of oil shale; however, a large amount of heavy components such as resin and asphaltene existed in the shale oil. This demonstrated that the solvent and driving effects of sub/supercritical water played a dominant role in the pyrolysis process of oil shale. The sub/supercritical water had the characteristics of higher diffusion coefficient, higher solvation energy and lower dielectric constant compared with natural water. Thus, sub/supercritical water have the ability to directly extract oil and gas from oil shale Also, they could weaken the bond energy between kerogen and the inherent minerals, thereby resulting in the dissociation and desorption of organic macromolecules from the inherent minerals. However, the thermal cracking of kerogen was still weak compared with high temperature pyrolysis, which led to the formation and release of

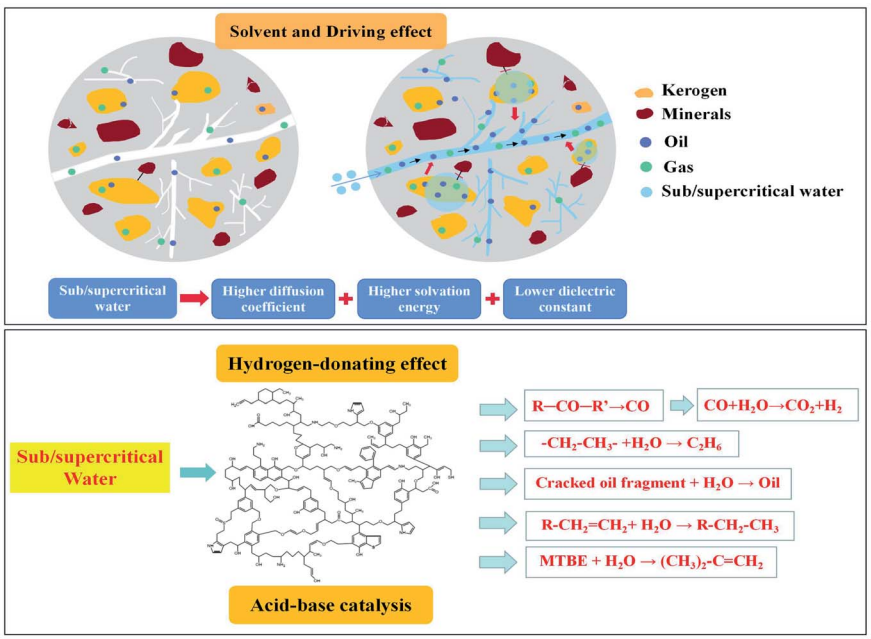

Fig. 11 Multiple mechanism of sub/supercritical water during the pyrolysis of oil shale.

macromolecule resin and asphaltene. Also, the sub/supercritical water as a heat carrier had a driving effect and enhanced the recovery rate of shale oil. This is because they could facilitate the migration of shale oil and carried the shale oil to rapidly escape from the pores and fractures, hindering their secondary cracking. Also, they also provided a homogeneous environment and reduced the viscosity of shale oil, thereby relieving the seepage resistance.

Furthermore, from the perspective of chemical reaction, sub/supercritical water could provide more hydrogen due to their higher ion product and induced more hydrogenation reactions. According to the results of pyrolysis gas, the increase of H_2 yield originated from the occurrence of a water gas shift reaction, where ethyl combines with hydrogen in sub/supercritical water to form ethane. Also, sub/supercritical water promoted the cracking and release of other small molecule gas. According to the results of shale oil, the macromolecule cracked oil fragments obtained from the extraction of sub/supercritical water combined with them and underwent a reforming reaction. The sub/supercritical water can be considered an acid–base catalyst, which can catalyze some reactions such as hydrolysis, addition, cracking, rearrangement, alcohol dehydration and carbenium reactions during the pyrolysis of oil shale. For example, in the shale oil, the C=C bonds in alkene underwent an addition reaction with sub/supercritical water to form more alkane under the catalysis of the acid–base catalyst. Also, methyl *tert*-butyl ether (MTBE) would be catalytically hydrolyzed to produce butene.[16] Sub/supercritical water also facilitated the cracking of the macromolecule oil fragments from kerogen.

Conclusions

(1) The existence of sub/supercritical water increased the mass loss of FS oil shale during pyrolysis and improved the release of oil and gas. The discharged oil yields from sub/supercritical water pyrolysis were 5.44 and 14.33 times than that from anhydrous pyrolysis at 360 °C and 450 °C, respectively, which was mainly due to their solvent effect. Also, the sub/supercritical water reduced the yield of residual oil and facilitated the migration of shale oil owing to their driving effect.

(2) The yields of H_2, CO_2 and hydrocarbons from sub/supercritical water pyrolysis were higher than that from anhydrous pyrolysis because of the chemical hydrogen-donating and acid–base catalytic effect. The water–gas shift reaction occurred during sub/supercritical water pyrolysis, resulting in an increase in the H_2 and CO_2 yields. Also, sub/supercritical water could promote the cracking of the aliphatic and aromatic side chains of kerogen, leading to an increase in hydrocarbon gas.

(3) The component of shale oil was dominated by saturated hydrocarbons in anhydrous pyrolysis, which accounted for 50–65%. In contrast, a large amount of asphaltenes and resins was generated in shale oil during sub/supercritical water pyrolysis due to the solvent effect and weak thermal cracking. The shale oil in anhydrous pyrolysis was lighter than that in sub/supercritical water pyrolysis, and the heavy fractions easily remained in the solid residuals.

(4) The sub/supercritical water reduced the indices of TOC and PC of the solid residuals and improved the cracking of organic matter in kerogen. The hydrocarbon generation potential of the solid residuals in anhydrous pyrolysis was superior to that in sub/supercritical water pyrolysis. The kerogen of the solid residuals gradually evolved from type I to type III as the temperature increased. The supercritical water reduced the T_{max} value and lowered the maturity of the solid residual.

Author contributions

Yang Lu: writing – original draft, methodology, formal analysis. Zhijing Wang: validation, formal analysis. Zhiqin Kang: conceptualization, resources. Wei Li: resources, supervision. Dong Yang: writing – review & editing, supervision. Yangsheng Zhao: project administration, funding acquisition.

Conflicts of interest

There are no conflicts to declare.

Acknowledgements

This work was supported by the National Key Research and Development Program of China (2019YFA0705501), China National Postdoctoral Program for Innovative Talents (Grant No. BX2021209) and China Postdoctoral Science Foundation (Grant No. 2021M692372).

References

1 H. Guo, Q. Cheng, Z. Jin, D. Wang, G. Xu and Y. Liu, *RSC Adv.*, 2016, **6**, 102231–102248.
2 T. Wu, Q. Xue, X. Li, Y. Tao, Y. Jin, C. Ling and S. Lu, *J. Supercrit. Fluids*, 2016, **107**, 499–506.
3 H. Lee, F. A. Shakib, K. Liu, B. Liu, B. Bubach, R. S. Varma, H. W. Jang, M. Shokouhimher and M. Ostadhassan, *RSC Adv.*, 2020, **10**, 23312–23320.
4 D. Lai, Y. Shi, S. Geng, Z. Chen, S. Gao, J. Zhan and G. Xu, *Fuel*, 2016, **173**, 138–145.
5 L. Lin, D. Lai, Z. Shi, Z. Han and G. Xu, *RSC Adv.*, 2017, **7**, 21467–21474.
6 Z. Chang, M. Chu, C. Zhang, S. Bai, H. Lin and L. Ma, *J. Anal. Appl. Pyrolysis*, 2018, **130**, 269–276.
7 Y. Lu, Y. Wang, Q. Wang, J. Zhang, Y. Zhao and Y. Zhang, *Fuel*, 2020, **267**, 117287.
8 C. Yu, Z. Qi, Y. Guo, J. Bian, X. Meng and Q. Long, *J. Anal. Appl. Pyrolysis*, 2020, **152**, 104942.
9 S. Wang, X. Jiang, X. Han and J. Tong, *Energy*, 2012, **42**, 224–232.
10 W. Guo, Q. Yang, Y. Sun, S. Xu, S. Kang, C. Lai and M. Guo, *J. Anal. Appl. Pyrolysis*, 2020, **146**, 104759.
11 Z. Kang, Y. Zhao and D. Yang, *Appl. Energy*, 2020, **269**, 115121.
12 D. Yang, L. Wang, Y. Zhao and Z. Kang, *J. Pet. Sci. Eng.*, 2021, **196**, 108101.

13 L. Wang, Y. Zhao, D. Yang, Z. Kang and J. Zhao, *Fuel*, 2019, **253**, 1490–1498.
14 M. Siskin and A. R. Katritzky, *Chem. Rev.*, 2001, **101**, 825–835.
15 G. Brunner, *J. Supercrit. Fluids*, 2009, **47**, 373–381.
16 N. Akiya and P. E. Savage, *Chem. Rev.*, 2002, **102**, 2725–2750.
17 M. Siskin and A. R. Katritzky, *Science*, 1991, **254**, 231–237.
18 S. Deng, Z. Wang, Y. Gao, Q. Gu, X. Cui and H. Wang, *J. Anal. Appl. Pyrolysis*, 2012, **98**, 151–158.
19 S. Kang, Y. Sun, M. Qiao, S. Li, S. Deng, W. Guo, J. Li and W. He, *Energy*, 2022, **238**, 121763.
20 H. R. Patrick, K. Griffith, C. L. Liotta, C. A. Eckert and R. Gläser, *Ind. Eng. Chem. Res.*, 2001, **40**, 6063–6067.
21 Y. Sun, S. Kang, S. Wang, L. He, W. Guo, Q. Li and S. Deng, *Energy Fuels*, 2019, **33**, 2106–2114.
22 W. Patrick, N. U. Clement, A. S. Lee, M. Will, E. S. Colin, H. V. Christopher, M. H. Vicky and D. C. Andrew, *Nat. Commun.*, 2019, **10**, 3659.
23 Y. Ma and S. Li, *Carbon Resour. Convers.*, 2018, **1**, 160–164.
24 Z. Wang, S. Deng, Q. Gu, X. Cui, Y. Zhang and H. Wang, *Energy Fuels*, 2014, **28**, 2305–2313.
25 M. D. Lewan and S. Roy, *Org. Geochem.*, 2011, **42**, 31–41.
26 K. E. harfi, C. Bennouna, A. Mokhlisse, M. B. chanâa, L. Lemée, J. Joffre and A. Amblès, *J. Anal. Appl. Pyrolysis*, 1999, **50**, 163–174.
27 Z. R. Nasyrova, G. P. Kayukova, A. V. Vakhin, R. Djimasbe and A. E. Chemodanov, *Processes*, 2020, **8**, 800.
28 M. Chen, Y. Shi, L. Dong and Q. Wang, *Oil Shale*, 2010, **27**, 297–308.
29 Q. Li, X. Han, Q. Liu and X. Jiang, *Fuel*, 2014, **121**, 109–116.
30 Y. Sun, F. Bai, B. Liu, Y. Liu, M. Guo, W. Guo, Q. Wang, X. Lü, F. Yang and Y. Yang, *Fuel*, 2014, **115**, 338–346.
31 F. Bai, W. Guo, X. Lü, Y. Liu, M. Guo, Q. Li and Y. Sun, *Fuel*, 2015, **146**, 111–118.
32 Y. You, X. Han, J. Liu and X. Jiang, *J. Therm. Anal. Calorim.*, 2018, **131**, 1845–1855.
33 X. Ru, Z. Cheng, L. Song, H. Wang and J. Li, *J. Mol. Struct.*, 2012, **1030**, 10–18.
34 J. G. Na, C. H. Im, S. H. Chung and K. B. Lee, *Fuel*, 2012, **95**, 131–135.
35 L. Wang, D. Yang and Z. Kang, *Fuel*, 2021, **290**, 119786.
36 J. D. Tucker, B. Masri and S. Lee, *Energy Sources*, 2000, **2**, 453–463.
37 Q. Zhao, L. Guo, Z. Huang, L. Chen, H. Jin and Y. Wang, *Energy Fuels*, 2018, **32**, 1685–1692.
38 Q. Zhao, L. Guo, Y. Wang, H. Jin, L. Chen and Z. Huang, *Energy Fuels*, 2020, **34**, 360–367.
39 S. Zhao, X. Lü, Q. Li and Y. Sun, *Chem. Eng. J.*, 2020, **394**, 125037.
40 S. Guo, L. Guo, J. Yin and H. Jin, *J. Supercrit. Fluids*, 2013, **78**, 95–102.
41 F. Huang and B. Hu, *RSC Adv.*, 2018, **8**, 38065–38074.
42 O. N. Fedyaeva, V. R. Antipenko, D. Y. Dubov, T. V. Kruglyakova and A. A. Vostrikov, *J. Supercrit. Fluids*, 2016, **109**, 157–165.
43 J. Hao, W. Feng, Y. Qiao, Y. Tian, J. Zhang and Y. Che, *Energy Convers. Manage.*, 2017, **151**, 227–239.
44 P. Krammer and H. Vogel, *J. Supercrit. Fluids*, 2000, **16**, 189–206.
45 J. Liu, X. Jiang, J. Shen and H. Zhang, *Energy Convers. Manage.*, 2014, **87**, 1027–1038.
46 T. Sato, T. Sumita and N. Itoh, *J. Supercrit. Fluids*, 2015, **104**, 171–176.
47 M. Wang, L. Jin, Y. Li, J. Lv, B. Wei and H. Hu, *Fuel Process. Technol.*, 2018, **177**, 119–128.
48 M. Golombok, *J. Chem. Educ.*, 2004, **81**, 228–231.
49 Z. Chang, M. Chu, C. Zhang, S. Bai, H. Li and L. Ma, *Korean J. Chem. Eng.*, 2017, **34**, 3111–3118.
50 Y. Yi, S. Li, F. Ding and H. Yu, *Pet. Sci.*, 2009, **6**, 194–200.
51 J. Li, M. Wang, Z. Chen, S. Lu, C. Jiang, G. Chen and S. Tian, *J. Anal. Appl. Pyrolysis*, 2019, **144**, 104707.
52 M. Li, Z. Chen, T. Cao, X. Ma, X. Liu, Z. Li, Q. Jiang and S. Wu, *Int. J. Coal Geol.*, 2018, **191**, 38–47.